

# Performance of the GenEst Mortality Estimator Compared to The Huso and Shoenfeld Estimators

---

## Final Report



### Prepared for:

**American Wind Wildlife Institute**

1990 K Street, NW, Suite 620  
Washington, DC 20006

---

### Prepared by:

**Paul A Rabie<sup>1</sup>, Daniel Riser-Espinoza<sup>1</sup>, Jared Studyvin<sup>1</sup>,**

**Daniel Daltorp<sup>2</sup>, and Manuela Huso<sup>2</sup>**

<sup>1</sup>Western EcoSystems Technology, Inc.  
1610 Reynolds Street  
Laramie, Wyoming 82072

<sup>2</sup>US Geological Survey Forest & Rangeland Ecosystem Science Center  
777 NW 9<sup>th</sup> Street Suite 400  
Corvallis, Oregon 97331

**September 23, 2020**



## **STUDY PARTICIPANTS**

Paul A Rabie	Project Manager and Biometrician
Daniel Riser-Espinoza	Biometrician
Jared Studyvin	Biometrician
Daniel Dalthorp	Statistician
Manuela Huso	Research Statistician
Julia Preston-Fulton	Technical Editor

## **REPORT REFERENCE**

Rabie, P. A., D. Riser-Espinoza, J. Studyvin, D. Dalthorp, and M. Huso. 2020. Performance of the GenEst Mortality Estimator Compared to The Huso and Shoenfeld Estimators. Draft Report. Prepared for The American Wind Wildlife Institute, Washington, DC. Prepared by Western EcoSystems Technologies, Inc. (WEST), Laramie, Wyoming and US Geological Survey Forest & Rangeland Ecosystem Science Center, Corvallis, Oregon. September 23, 2020.

## TABLE OF CONTENTS

1	INTRODUCTION.....	1
2	METHODS .....	2
2.1	Mortality Estimation Components .....	2
2.2	Estimator Variants .....	4
2.3	Simulation Conditions.....	4
2.4	Estimator Implementation .....	6
2.5	Estimator Assessment.....	6
3	RESULTS.....	7
3.1	Bias .....	7
3.2	Confidence Interval Coverage .....	10
3.3	Precision and Confidence Interval Coverage.....	14
4	Implications for the Analysis and Design of Post-construction Monitoring Studies .....	22
5	LITERATURE CITED .....	24

## LIST OF TABLES

Table 1.	Factors and their values used in the simulations, and their descriptions.....	5
Table 2.	Parameter values and modeled detection probabilities for the five estimators. $p$ refers to initial searcher efficiency and $k$ to the detection reduction factor. <i>Persistence distributions</i> are parameterized as in the base R software. <i>mean CP:SI</i> is the mean carcass persistence time (itself a function of the persistence distribution) divided by the search interval (seven days in all cases). <i>mean CP:SI</i> less than 1.0 implies the search interval is longer than the mean persistence time and <i>mean CP:SI</i> greater than 1.0 implies the search interval is shorter than the mean persistence time.....	8

## LIST OF FIGURES

Figure 1.	Relative bias of the five estimators under the 36 core scenarios that result in different detection probabilities. Within each panel, the x-axis repeats the $k$ values twice. The y-axis has been log-transformed so an underestimate by a factor of 2 is visually similar to an overestimate by a factor of 2. The reference line at 1.0 indicates an unbiased estimator, points above the line suggest estimators biased high, and points below the line suggest estimators biased low. Dotted reference lines indicate estimates 0.8 and 1.2 times the unbiased value. ....	11
-----------	---	----

Figure 2. Confidence interval (CI) coverage of the five estimators under different bias trial sample sizes (in columns). Within each panel, the realized coverage is plotted from low to high across all simulations we conducted. Nominal coverage is indicated with a brown line at 0.9 and the shaded region includes coverage from 0.8 to 0.95. The top row of panels includes all simulations, the second row excludes simulations for which the expected carcass count was less than 2.3 per stratum (road and pad or cleared plots), and the third row additionally excludes simulations with sampling inadequate to capture the variability in mortality rates across the facility (see text).....12

Figure 3. Precision and confidence Interval (CI) coverage of mortality estimates in response to total mortality and sample size for bias trials. Boxplots show the median (horizontal bar), 25<sup>th</sup> and 75<sup>th</sup> quantiles (lower and upper bounds of the boxes) and 5<sup>th</sup> and 95<sup>th</sup> quantiles (whiskers) of the widths of 90% CI for mortality estimates. CI coverage is indicated in blue on the right axis and with asterisks, with a reference line indicating 90% coverage. The figure includes simulations for which there was a gradient of mortality across the 100-turbine wind facility. Sampling fraction was 100% with 30% of turbines searched as cleared plots and 70% as road and pads,  $p = 0.8$ ,  $k = 0.7$ , and carcass persistence was Weibull distributed with mean persistence time equal to the search interval. ....16

Figure 4. Precision and coverage of mortality estimates due to the carcass persistence time distribution,  $k$  and  $p$ . Boxplot interpretation as in Figure 3. The figure includes simulations for which total fatality was 1,000 individuals with a gradient of mortality across the 100-turbine wind facility. Sampling fraction was 100% with 30% of turbines searched as cleared plots and 70% as road and pads. Mean carcass persistence time was equal to the search interval. There were 50 bias trial carcasses available to estimate model parameters. ....17

Figure 5. Precision and coverage of mortality estimates due to the length of the mean carcass persistence time relative to the search interval,  $k$  and  $p$ . Boxplot interpretation as in Figure 3. The figure includes simulations for which total fatality was 1,000 individuals with a gradient of mortality across the 100-turbine wind facility. Sampling fraction was 100% with 30% of turbines searched as cleared plots and 70% as road and pads; carcass persistence was Weibull distributed. There were 50 bias trial carcasses available to estimate model parameters. ....18

Figure 6. Precision and coverage of mortality estimates due to spatial distribution of fatalities, sampling fraction, and total number of turbines at the facility. Boxplot interpretation as in Figure 3. The figure includes simulations for which total fatality was 1,000 individuals. Thirty percent of searched turbines were searched as cleared plots and 70% as road and pads,  $p = 0.8$ ,  $k = 0.7$ , and carcass persistence was Weibull distributed with mean persistence time equal to the search interval. There were 50 bias trial carcasses available to estimate model parameters. ....20

Figure 7. Precision and coverage of mortality estimates due to the plot configuration, sampling fraction, and total number of turbines at the facility. Boxplot interpretation as in Figure 3. The figure includes simulations for which total fatality was 1,000 individuals with a gradient of mortality across the wind facility,  $p = 0.8$ ,  $k = 0.7$ , and carcass persistence was Weibull distributed with mean persistence time equal to the search interval. There were 50 bias trial carcasses available to estimate model parameters. ....21

## 1 INTRODUCTION

The impacts of wind power development on bat and bird populations are commonly assessed by estimating the number of fatalities at wind power facilities through post-construction monitoring (PCM) studies. Standard methodology involves periodic carcass searches on plots beneath turbines (Strickland et al. 2011, US Fish and Wildlife Service 2012). The resulting counts are adjusted to compensate for bias due to imperfect carcass detection by searchers, removal of carcasses by scavengers or other processes (Korner-Nievergelt et al. 2011), and carcasses that may have fallen outside of searched areas. To account for the bias in counts due to imperfect detection and carcass removal, investigators typically conduct bias trial experiments to inform models of carcass detection probability. Many different estimators have been proposed that combine information about the bias trial experiments to estimate a detection probability for carcasses ( $g$ ) and ultimately obtain an estimate of total mortality ( $M$ ). The two estimators that have seen the most widespread use in North America recently are the Huso (Huso 2011, Huso et al. 2012) and Shoenfeld (Shoenfeld 2004; also called the Erickson estimator) estimators. GenEst (Dalthorp et al. 2018a, 2018b, 2018c) is the newest statistical estimator to become available and was designed to improve upon the Huso and Shoenfeld estimators by generalizing the key assumptions in both, and to improve comparability among new PCM studies. In addition to relaxing some of the assumptions inherent to the Huso and Shoenfeld estimators, GenEst uses a novel approach to variance estimation through a parametric bootstrap (Madsen et al. 2019).

The current study was undertaken to document the performance of GenEst relative to the Huso and Shoenfeld estimators. We took a simulation approach to the study because simulation data provides the basis to compare mortality estimators under conditions where the “truth” is known. The estimators were compared on three metrics: 1) bias—the tendency of an estimator to over- or under-estimate mortality, 2) precision—the ability of an estimator to constrain an estimate to a narrow range (measured here as the width of a 90% confidence interval [CI] around the point estimate divided by the true, known mortality rate), and 3) CI coverage—the probability a CI with a specified level of confidence actually includes the true level of mortality.

Although our simulations were conceived and designed—and are discussed—with respect to wind farms, it is important to note that the estimators and results discussed here are relevant to any post-construction mortality monitoring study that may occur (such as at solar facilities) where detection is imperfect. Although our study treats the problem of mortality estimation when detection is imperfect, it is also important to note that all of the estimators considered here are Horvitz-Thompson (Horvitz and Thompson 1952) style estimators, that is, none are designed to estimate the mortality of rare species as might be necessary under an Incidental Take Permit. The Evidence of Absence estimator (Dalthorp et al. 2017) is still the most appropriate statistical tool for rare event estimation.

The simulations cover a broad range of conditions that may occur in field studies and complete results are presented without commentary in the appendix. The main body of this report does not provide a comprehensive treatment of our results; rather, we try to identify some of the more

important differences among the estimators and some conditions under which reliable mortality estimates are especially challenging.

## 2 METHODS

### 2.1 Mortality Estimation Components

All of the estimators treated here address four or five of the same components of carcass detection probability to arrive at an estimate of total mortality, and differ primarily in the assumptions associated with the components of detection probability. We begin with a brief review of these components.

The *carcass persistence probability* addresses the potential bias in carcass counts due to the fact that a carcass may be removed by a scavenger (or another process) before a searcher completes a monitoring survey. The GenEst and Huso estimators both use survival-modeling techniques to estimate a distribution of carcass persistence times, from which the average persistence probability can be calculated. These estimators provide the user with tools to help choose among different distributions for carcass persistence times, which makes them flexible with respect to the carcass persistence dynamics. The Shoenfeld estimator implicitly assumes carcass persistence times follow an exponential distribution. When persistence times do not meet this assumption, the Shoenfeld estimator can be biased.

*Searcher efficiency* addresses the bias that arises from imperfect detection of carcasses by searchers. All of the estimators tested here take an initial searcher efficiency parameter ( $p$ ), which may differ from season to season or between substrate strata at a wind farm. Searcher efficiency also depends on carcass age, as carcasses tend to become more difficult to discover as they age, and  $k$  describes how searcher efficiency changes as carcasses age. Carcasses newly arrived at a facility may be detected with probability  $p$  (above) or may be missed. Those carcasses that are missed may begin to disintegrate and become harder to detect, or may have been well concealed in the first place, so it is reasonable to expect that a carcass that has been missed once will have a lower detection probability than a fresh carcass. The  $k$  parameter describes how searcher efficiency changes through multiple searches.

Shoenfeld assumes searcher efficiency does not depend on carcass age ( $k = 1$ ). Huso assumes carcasses that are not discovered in the first search after arrival cannot be discovered in later searches, i.e., searcher efficiency goes to zero for carcasses missed in the first search ( $k = 0$ ). Among the estimators tested here, only GenEst treats  $k$  explicitly. GenEst uses a maximum likelihood procedure to estimate  $p$  simultaneously with  $k$ , if there are multiple search data available (as in our *GenEst-est k* estimations below). If there are only single-search data available, the GenEst estimation routine to estimate  $p$  reduces to a logistic regression, and the user must specify a value (between zero and one) for  $k$  (as in our *GenEst-fixed k* simulations below, which used a fixed value of 0.7 for  $k$ ). Choosing fixed  $k = 1$  is equivalent to the Shoenfeld approach to modeling searcher efficiency, and choosing fixed  $k = 0$  is equivalent to the Huso approach. The Huso estimator uses logistic regression to estimate  $p$ , and although there is no canonical approach to

estimating  $p$  for the Shoenfeld estimator, logistic regression is a reasonable choice and was used here.

The estimators behave differently when presented with a data set for which either all or none of the searcher efficiency trial carcasses are detected. When no searcher efficiency trial carcasses are detected by searchers, the Shoenfeld and Huso estimators are unable to produce a mortality estimate because with  $p = 0$ , estimated mortality would be infinite, which is nonsensical. In contrast, the GenEst estimator (version 1.3.1 and later) uses an estimate of  $1 / (2 * n)$  when no searcher efficiency trial carcasses are detected (e.g., if all of 10 carcasses are missed, GenEst will use an assumed value of 1/20 for  $p$ ). Although this assumption introduces an unknown bias to the estimator, it allows GenEst to produce mortality estimates where other estimators fail. When all searcher efficiency trial carcasses are detected by searchers, the Shoenfeld and Huso estimators proceed with a searcher efficiency estimate of 1.0, which is also implausible and introduces an unknown bias, but perhaps not an unreasonable approximation of reality if the number of trial carcasses is large. Analogous to the zero-found case, the GenEst estimator (as of version 1.3.1) assumes searcher efficiency is  $1 - 1 / (2 * n)$  when all carcasses are found (e.g., if all of 10 trial carcasses are detected, GenEst will use an assumed value of 19/20 for  $p$ ). This assumption introduces an unknown bias to the estimator, but in most cases will be less biased than simply assuming  $p = 1$  and gives a more realistic assessment of the uncertainty in the estimate of  $p$  (and total mortality) when all searcher efficiency carcasses are detected.

A final important difference between the estimators is the treatment of uncertainty. Shoenfeld (2003) did not address uncertainty in the estimator. The Huso estimator uses a non-parametric bootstrap (i.e., a data-resampling procedure) to capture uncertainty in the detection probability and carcass counts, and we use the same approach for the Shoenfeld estimator. The GenEst estimator uses a parametric bootstrap procedure to capture uncertainty in the detection probability and carcass counts. For detection probability, this means parameter estimates are resampled based on the estimated uncertainty in the model; for carcass counts, the parametric bootstrap represents a completely novel approach developed specifically for the GenEst model (though it potentially has much wider application; Madsen et al. 2019). A consequence of the parametric bootstrap used by GenEst is that rather than the turbine being a statistical sample unit (as in the Huso and Shoenfeld estimators), the carcass is the sample unit, which frees GenEst from the assumption that mortality rates are constant among turbines and makes it applicable across a broader range of conditions.

Differences in the way carcass persistence, searcher efficiency,  $k$ , and uncertainty are treated mark the most fundamental differences between the estimators tested here, but two other components of mortality estimation are also important and were included in our simulation. *Sampling fraction* refers to the fraction of wind turbines at a farm actually subject to search and is an important indicator of the actual sampling effort. The sampling effort also depends on plot configurations. Large, cleared plots may be expected to capture most carcasses that arrive at a wind farm, whereas road and pad searches that are restricted to the graveled surfaces around wind turbines may capture a small fraction of the total carcasses that arrive. The fraction of



carcasses expected to occur within searched areas is called the *density-weighted proportion of area searched*, or DWP.

The estimated detection probabilities for all of the estimators treated here are adjusted after the fact to account for sampling fraction and DWP. *Post hoc* adjustment for sampling fraction and DWP means their effects on the point estimates of mortality scale linearly with sampling fraction and DWP, but because the different estimators handle uncertainty associated with carcass counts differently, these factors can impact precision and CI coverage differently for the different estimators.

## **2.2 Estimator Variants**

The study tested estimator performance of five estimator variants (italicized below) under a variety of simulated conditions (Table 1). Three estimators were tested: the GenEst estimator (as in version 1.4.2 of the software), the Huso estimator, and the Shoenfeld estimator. GenEst has the capacity to estimate the proportional change in searcher efficiency with each successive search ( $k$ ) or to treat it as fixed and known. For the *GenEst-est  $k$*  case, we estimated  $k$  from simulated bias trial data. For the *GenEst-fixed  $k$*  case, we assumed  $k$  was equal to 0.7, regardless of its actual value. The Huso estimator includes the implicit assumption that  $k$  is zero, which is to say it assumes that if a carcass is missed once it will never be detected. Carcass search data can be prepared to approximate this assumption by restricting the carcass counts to only those carcasses that are ‘fresh,’ i.e., occurred since the last search. The notion that carcasses can be censored to satisfy the assumptions of the Huso estimator is simple in principle but it bears emphasizing that in the field, the task of censoring carcasses is influenced by a great deal of subjective judgment, and accuracy in the censoring process remains untested. *Huso-censored* estimates were calculated using carcass counts identified as fresh (with perfect accuracy), and *Huso-not censored* estimates used all carcasses in the estimates. Neither of our Huso variants is likely to be the case in the field but they represent a range of potential outcomes. The *Shoenfeld* estimator makes the implicit assumption that  $k$  is 1.0, which means the detection probability for a carcass never changes, regardless of how many times it has been missed. Unlike the Huso estimator, there is no way to prepare the data so it matches the implicit assumptions of the Shoenfeld estimator. Thus, the three basic estimators resulted in five types of mortality estimates: *GenEst-est  $k$* , *GenEst-fixed  $k$* , *Huso-censored*, *Huso-not censored*, and *Shoenfeld*.

## **2.3 Simulation Conditions**

Several factors affect the performance of these estimators. The factors that we consider are total mortality at a site, whether the mortality is evenly distributed among turbines or varies among turbines, the number of turbines at a site, the sampling fraction, the DWP (which depends on plot configuration), the carcass persistence distribution, the length of the search interval relative to the average carcass persistence time, the searcher efficiency, the value of  $k$ , and, finally, the number of trial carcasses used to estimate  $p$ ,  $k$ , and carcass persistence.

Each estimator was tested in the context of simulated mortality monitoring studies at a wind facility. The simulated studies covered 26 weeks with the search interval fixed at seven days. All simulated fatalities were assumed to be from the same class of animals in terms of detection and

persistence probability (i.e., all bats or all similarly sized birds). The total number of fatalities arriving at the wind facility, carcass persistence distribution, mean persistence time, searcher efficiency, number of bias trial carcasses, distribution of fatalities across the wind facility, and  $k$  were varied systematically across the simulations—see Table 1 for a description of all conditions tested during simulations. All combinations of conditions in Table 1 were simulated for each estimator, except for the combination of a uniform distribution of total mortality  $M= 10$  at a site with 100 turbines because it is impossible to uniformly distribute 10 whole carcasses across 100 turbines. There were 4,752 simulation scenarios to which each of the five estimators was applied. A carcass count and bias trial data were generated 1000 times for each of the 4,752 scenarios. For each carcass count, each estimator gave a point estimate of mortality ( $\hat{M}$ ) and a 90% CI around  $\hat{M}$ .

**Table 1. Factors and their values used in the simulations, and their descriptions.**

<b>Factor</b>	<b>Levels</b>	<b>Description</b>
Total mortality (M) at a site	M = 1000 M = 100 M = 10	Total number of carcasses distributed at simulated wind facilities.
Spatial distribution of mortality	Uniform M  Variable M	Uniform M distribution indicates the case where the mortality rates are identical for all turbines at a facility.  Variable M distribution indicates the case where the mortality rates at turbines within a wind facility included a five-fold variation from the least lethal turbine to the most lethal turbine.
Number of turbines	100 turbines 10 turbines	Number of turbines over which to distribute total fatalities.
Sampling fraction (f)	f = 1.0 f = 0.3	Proportion of total turbines at a facility that were searched.
Plot configurations	Plot type = Cleared Plot type = Cleared + RP	Plot configuration for searches involved either cleared plots at all searched turbines (assumed large enough to capture all carcasses) or a mixture of 30% cleared plots and 70% of turbines searched on road and pads (large enough to capture 15% of carcasses).
Carcass persistence time distribution <sup>1</sup>	Exponential Weibull	Carcass persistence times followed either an exponential distribution or a Weibull distribution with a shape parameter equal to 0.6.
Ratio of average persistence time to search interval	Mean CP:SI = 1/3 Mean CP:SI = 1 Mean CP:SI = 3	Ratio of average carcass persistence time:length of search interval; these resulted in probability of persisting through the search interval ( $r$ ) being 21%, 33% and 27% higher for the exponential than Weibull, respectively .
Searcher efficiency for a fresh carcass	p = 0.8 p = 0.2	Probability a fresh carcass will be detected on a search, assuming it has not been removed
Detection reduction factor (k)	k = 0 k = 0.7 k = 1.0	Fraction by which searcher efficiency for an aging carcass decreases with each successive search.
Number (N) of bias trial carcasses	N bias trials = Infinite N bias trials = 50 N bias trials = 10	Mortality estimators are informed by bias trials to estimate searcher efficiency, carcass persistence (and for GenEst, $k$ ). We simulated 10 or 50 bias trials, and the ideal case

		where components of bias were known with certainty (N bias trials = infinite).
Estimator	GenEst-est k GenEst-fixed k Huso-censored Huso-not censored Shoenfeld	See text above.

---

## 2.4 Estimator Implementation

Estimates and CIs (parametric) for *GenEst-est k* and *GenEst-fixed k* were generated using version 1.4.2 of the GenEst R package. For the *Huso-censored*, and *Huso-not censored*, estimates and CIs were generated using R code adapted from US Geological Survey Data Series 729 (Huso et al. 2012), and, thus, replicate the expected behavior of the Huso estimator as implemented in Data Series 729. There is no R package or publicly available software for implementing the Shoenfeld estimator, and critical details of the implementation of the estimator can vary considerably from project to project. The estimates for *Shoenfeld* were generated using R code developed by WEST based on Shoenfeld (2004). CIs for the Huso and Shoenfeld estimators were generated using a non-parametric bootstrap approach similar to that used in Data Series 729. For the Huso and Shoenfeld estimator variants, no estimate was produced for a simulation iteration when zero searcher efficiency carcasses were found on the first search of the associated simulated bias trials, although in DS 729 a minimum SE of 1/20 is assumed in such cases. GenEst version 1.3.1 and later assumes  $p = 1 / (2 * n)$  in these cases.

## 2.5 Estimator Assessment

Estimator performance was assessed based on three metrics: CI coverage, relative bias, and precision. CI coverage is calculated as the proportion of the 1000 simulated 90% CIs around  $\hat{M}$  that contain the true mortality,  $M$ . That the 90% CI actually achieve nominal coverage, i.e., that it includes  $M$  90% of the time, is important for correct interpretation of results. A 90% CI that contains the true  $M$  100% of the time would be easy to construct, e.g.,  $M$  is between what was found and some very large number, 1,000,000 say, but would be of little practical value. Conversely, a very narrow CI might look appealing from a precision perspective, but, again, would be of little value if it never included the true value of  $M$ . The relative bias is calculated as the estimated mortality ( $\hat{M}$ ) divided by the true mortality  $M$ . The ratio equals 1.0 when the estimate is identical to the true mortality, is greater than 1.0 for estimates above the true  $M$ , and less than 1.0 for estimates below the true  $M$ . Relative bias of  $\frac{1}{2}$  is equivalent to bias of 2 in terms of how far the estimator misses the mark. Precision is calculated as the width of the 90% CI around the estimate of  $M$  divided by the true mortality  $M$ . We chose to standardize this metric, analogously to a coefficient of variation, to facilitate comparison of precision across different levels of true mortality.

None of the three metrics can be interpreted well by itself. For example, an estimator may be unbiased, i.e., its average value over the 1000 iterations is exactly the true mortality, but it may also be very imprecise with 90% CIs so large that they cover the true mortality 100% of the time. An estimator with this characteristic is unlikely to be of practical use. An estimator may, on the

other hand, be extremely precise, but the 90% CIs so narrow that they rarely include the true mortality. The best estimator will be one that is consistently accurate (relative bias = 1), precise, and achieves nominal coverage. To present the results in a manageable way, we begin with a discussion of the inherent biases of the estimators, followed by a high-level overview of CI coverage, and then a series of results for which we discuss precision and coverage simultaneously.

### **3 RESULTS**

#### **3.1 Bias**

The Huso, GenEst, and Shoenfeld estimators differ most profoundly in the parameters used in estimating overall detection probability and the assumptions on which those detection probability models are based. We begin by analyzing the 36 core scenarios that include all combinations of the searcher efficiency,  $k$ , and carcass persistence parameters that we investigated. For this analysis, we ignore the factors that primarily affect the assessments of uncertainty (total mortality, the spatial dispersion of carcasses among turbines, the number of turbines, and the number of field trial carcasses) and the extrapolation factors (DWP and sampling fraction), which the three estimators handle in similar ways.

Table 2 gives the modeled probability of detection ( $g$ ) for each of the five estimators, assuming the sampling fraction and density-weighted proportion of carcasses are both 1.0 under the 36 core scenarios. The 36 unique simulation scenarios derive from two levels of searcher efficiency (0.2 and 0.8), three levels of  $k$  (0, 0.7 and 1.0), two carcass persistence distributions (Exponential and Weibull), and three mean carcass persistence times relative to search interval (1/3, 1, 3). The modeled detection probabilities for GenEst with known  $k$  and for Huso with perfect carcass censoring are exactly correct, but they differ from one another when  $k$  is not zero because they assume different data collection procedures in the field. The Huso estimator is unbiased when  $k = 0$  or when carcasses are accurately censored, but biased by a factor of  $\frac{g_{GenEst}}{g_{Huso}}$  when  $k$  is greater than zero and carcasses are not censored.

Table 2. Parameter values and modeled detection probabilities for the five estimators. *p* refers to initial searcher efficiency and *k* to the detection reduction factor. *Persistence distributions* are parameterized as in the base R software. *Mean CP:SI* is the mean carcass persistence time (itself a function of the persistence distribution) divided by the search interval (seven days in all cases). *Mean CP:SI* less than 1.0 implies the search interval is longer than the mean persistence time and *mean CP:SI* greater than 1.0 implies the search interval is shorter than the mean persistence time.

Estimator parameters				Modeled detection probabilities			
<i>p</i>	<i>k</i>	Persistence distribution (parameters)	Mean CP:SI	GenEst-k known	GenEst-k assumed to be 0.7	Huso (both variants)	Shoenfeld
0.8	1.0	exponential (rate = 0.0476)	3.00	0.789	0.766	0.680	0.794
0.8	1.0	exponential (rate = 0.1429)	1.00	0.544	0.534	0.506	0.546
0.8	1.0	exponential (rate = 0.4286)	0.33	0.256	0.255	0.253	0.256
0.8	1.0	Weibull (shape = 0.6; scale = 13.9574)	3.00	0.615	0.599	0.537	0.794
0.8	1.0	Weibull (shape = 0.6; scale = 4.6525)	1.00	0.415	0.406	0.380	0.546
0.8	1.0	Weibull (shape = 0.6; scale = 1.5287)	0.33	0.217	0.215	0.210	0.256
0.8	0.7	exponential (rate = 0.0476)	3.00	0.766	0.766	0.68	0.794
0.8	0.7	exponential (rate = 0.1429)	1.00	0.534	0.534	0.506	0.546
0.8	0.7	exponential (rate = 0.4286)	0.33	0.255	0.255	0.253	0.256
0.8	0.7	Weibull (shape = 0.6; scale = 13.9574)	3.00	0.599	0.599	0.537	0.794
0.8	0.7	Weibull (shape = 0.6; scale = 4.6525)	1.00	0.406	0.406	0.380	0.546
0.8	0.7	Weibull (shape = 0.6; scale = 1.5287)	0.33	0.215	0.215	0.210	0.256
0.8	0	exponential (rate = 0.0476)	3.00	0.680	0.766	0.680	0.794
0.8	0	exponential (rate = 0.1429)	1.00	0.506	0.534	0.506	0.546
0.8	0	exponential (rate = 0.4286)	0.33	0.253	0.255	0.253	0.256
0.8	0	Weibull (shape = 0.6; scale = 13.9574)	3.00	0.537	0.599	0.537	0.794
0.8	0	Weibull (shape = 0.6; scale = 4.6525)	1.00	0.380	0.406	0.380	0.546
0.8	0	Weibull (shape = 0.6; scale = 1.5287)	0.33	0.210	0.215	0.210	0.256
0.2	1.0	exponential (rate = 0.0476)	3.00	0.378	0.284	0.170	0.399
0.2	1.0	exponential (rate = 0.1429)	1.00	0.176	0.158	0.126	0.179
0.2	1.0	exponential (rate = 0.4286)	0.33	0.066	0.065	0.063	0.066
0.2	1.0	Weibull (shape = 0.6; scale = 13.9574)	3.00	0.298	0.220	0.134	0.399
0.2	1.0	Weibull (shape = 0.6; scale = 4.6525)	1.00	0.151	0.128	0.095	0.179
0.2	1.0	Weibull (shape = 0.6; scale = 1.5287)	0.33	0.062	0.059	0.052	0.066
0.2	0.7	exponential (rate = 0.0476)	3.00	0.284	0.284	0.170	0.399
0.2	0.7	exponential (rate = 0.1429)	1.00	0.158	0.158	0.126	0.179
0.2	0.7	exponential (rate = 0.4286)	0.33	0.065	0.065	0.063	0.066
0.2	0.7	Weibull (shape = 0.6; scale = 13.9574)	3.00	0.220	0.220	0.134	0.399
0.2	0.7	Weibull (shape = 0.6; scale = 4.6525)	1.00	0.128	0.128	0.095	0.179
0.2	0.7	Weibull (shape = 0.6; scale = 1.5287)	0.33	0.059	0.059	0.052	0.066
0.2	0	exponential (rate = 0.0476)	3.00	0.170	0.284	0.170	0.399

Table 2. Parameter values and modeled detection probabilities for the five estimators.  $p$  refers to initial searcher efficiency and  $k$  to the detection reduction factor. *Persistence distributions* are parameterized as in the base R software. *Mean CP:SI* is the mean carcass persistence time (itself a function of the persistence distribution) divided by the search interval (seven days in all cases). *Mean CP:SI* less than 1.0 implies the search interval is longer than the mean persistence time and *mean CP:SI* greater than 1.0 implies the search interval is shorter than the mean persistence time.

Estimator parameters				Modeled detection probabilities			
$p$	$k$	Persistence distribution (parameters)	Mean CP:SI	GenEst-k known	GenEst-k assumed to be 0.7	Huso (both variants)	Shoenfeld
0.2	0	exponential (rate = 0.1429)	1.00	0.126	0.158	0.126	0.179
0.2	0	exponential (rate = 0.4286)	0.33	0.063	0.065	0.063	0.066
0.2	0	Weibull (shape = 0.6; scale = 13.9574)	3.00	0.134	0.220	0.134	0.399
0.2	0	Weibull (shape = 0.6; scale = 4.6525)	1.00	0.095	0.128	0.095	0.179
0.2	0	Weibull (shape = 0.6; scale = 1.5287)	0.33	0.052	0.059	0.052	0.066

Figure 1 shows that the *GenEst-est k* and the *Huso-censored* estimators are unbiased under all 36 combinations. *GenEst-fixed k* becomes biased when *k* is mis-specified: when *k* is assumed higher than the real value, *GenEst-fixed k* becomes biased low, and when it is assumed lower than the real value, *GenEst-fixed k* becomes biased high. Low values of *p* and long carcass persistence times relative to the search interval cause the greatest degree of bias in *GenEst-fixed k* with mis-specified values of *k*. The *Huso-not censored* estimator is unbiased only in the unlikely event that the true value of *k* is zero (i.e., there really is only one chance to detect a carcass in the field). When *k* is greater than zero, the *Huso-not censored* estimator is biased high. Higher values of *k*, lower values of *p*, and long persistence times relative to the search interval cause the greatest degree of bias in the *Huso-not censored* estimator. In most cases, (and all cases tested here), the *Shoenfeld* estimator is biased low because it implicitly assumes 1) *k* is 1.0, 2) carcass persistence times are exponentially distributed, and 3) each carcass is subject to an infinite number of searches. Thus, even in the unlikely situation where *k* is 1.0 (i.e., carcasses are equally detectable after any number of searches), the *Shoenfeld* estimator slightly underestimates fatalities. Underestimates are more pronounced with smaller values of *k*, with lower values of *p*, and with shorter persistence times relative to the searcher interval. For the carcass persistence distributions tested here, the underestimates by the *Shoenfeld* estimator are more pronounced with Weibull-distributed carcass persistence times than with exponentially distributed carcass persistence times. This outcome is because the Weibull shape parameter we used (0.6) implies more rapid removal of fresh carcasses compared to exponentially distributed persistence times, but this result is not necessarily true for all possible Weibull-distributed carcass persistence dynamics.

### **3.2 Confidence Interval Coverage**

CI coverage refers to the probability a CI will include the true value of a parameter that is being estimated. Ideally, an estimator should produce CIs with nominal coverage—i.e., ideally a 90% CI should include the truth with 90% probability. CI coverage greater than nominal suggests CIs are too wide. CI coverage less than nominal can be due to estimators that are “missing” variance (CIs too narrow), or to bias (systematic over- or under- estimation) in the estimators.

There are some easily identified conditions under which no Horvitz-Thompson estimators consistently achieve nominal coverage. Figure 2 illustrates these. The figure is organized into three columns according to the precision with which detection probability is estimated. In the left column (infinite bias trials), the detection probability is known exactly and without error, the center column presents results from simulations in which 50 bias trial carcasses were used to estimate carcass persistence and searcher efficiency models, and the right column presents results from simulations using 10 bias trial carcasses. In all panels, the actual CI coverage associated with simulation conditions was sorted from low to high for each estimator and plotted as a line. An ideal estimator would be represented by a horizontal line on top of the reference line at 90% CI coverage. The longer an estimator’s line is within the shaded area (representing 80% - 95% coverage), the better its coverage property. The three rows in Figure 2 represent successive elimination of conditions under which no Horvitz-Thompson estimator can achieve good coverage.

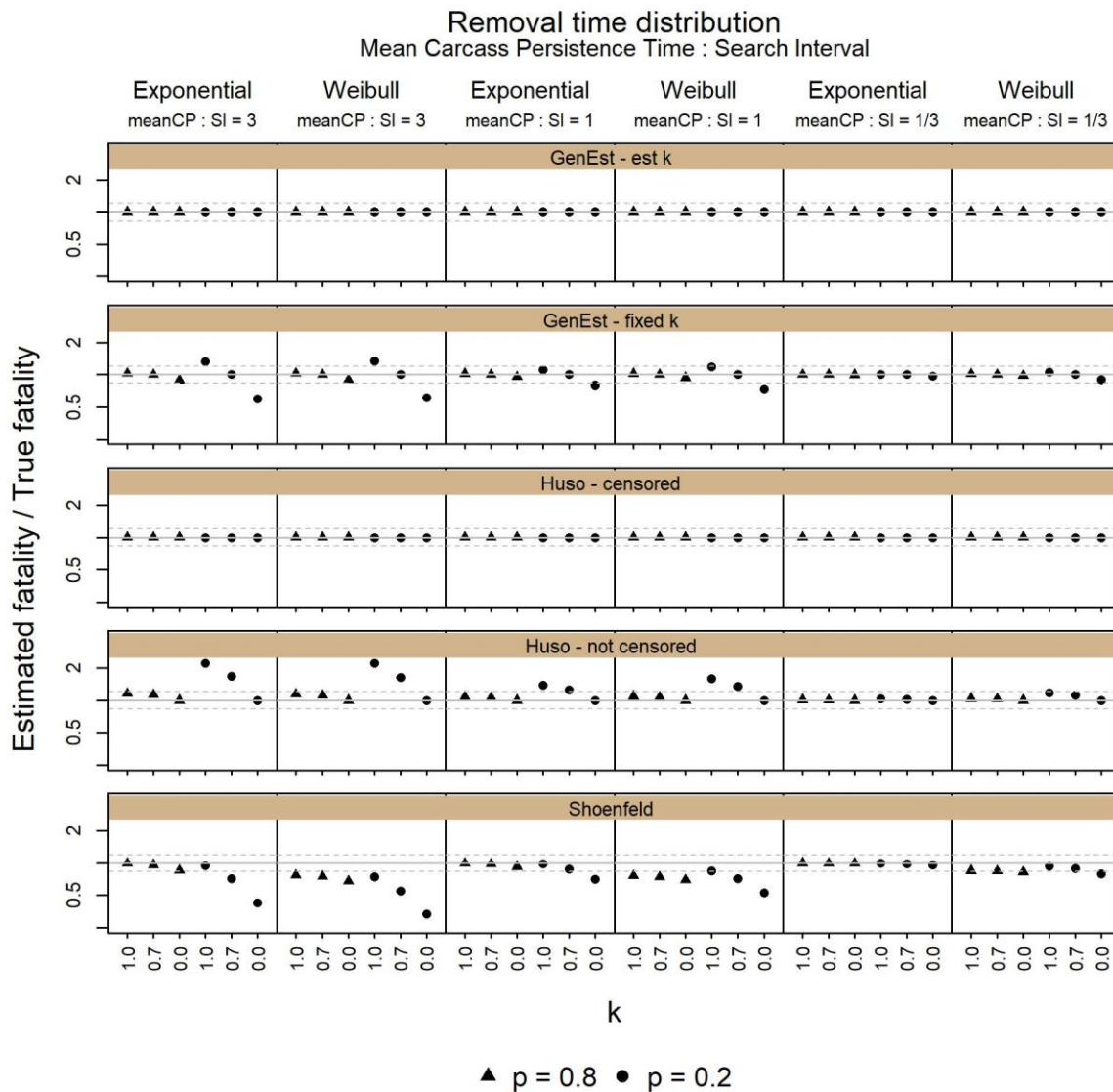
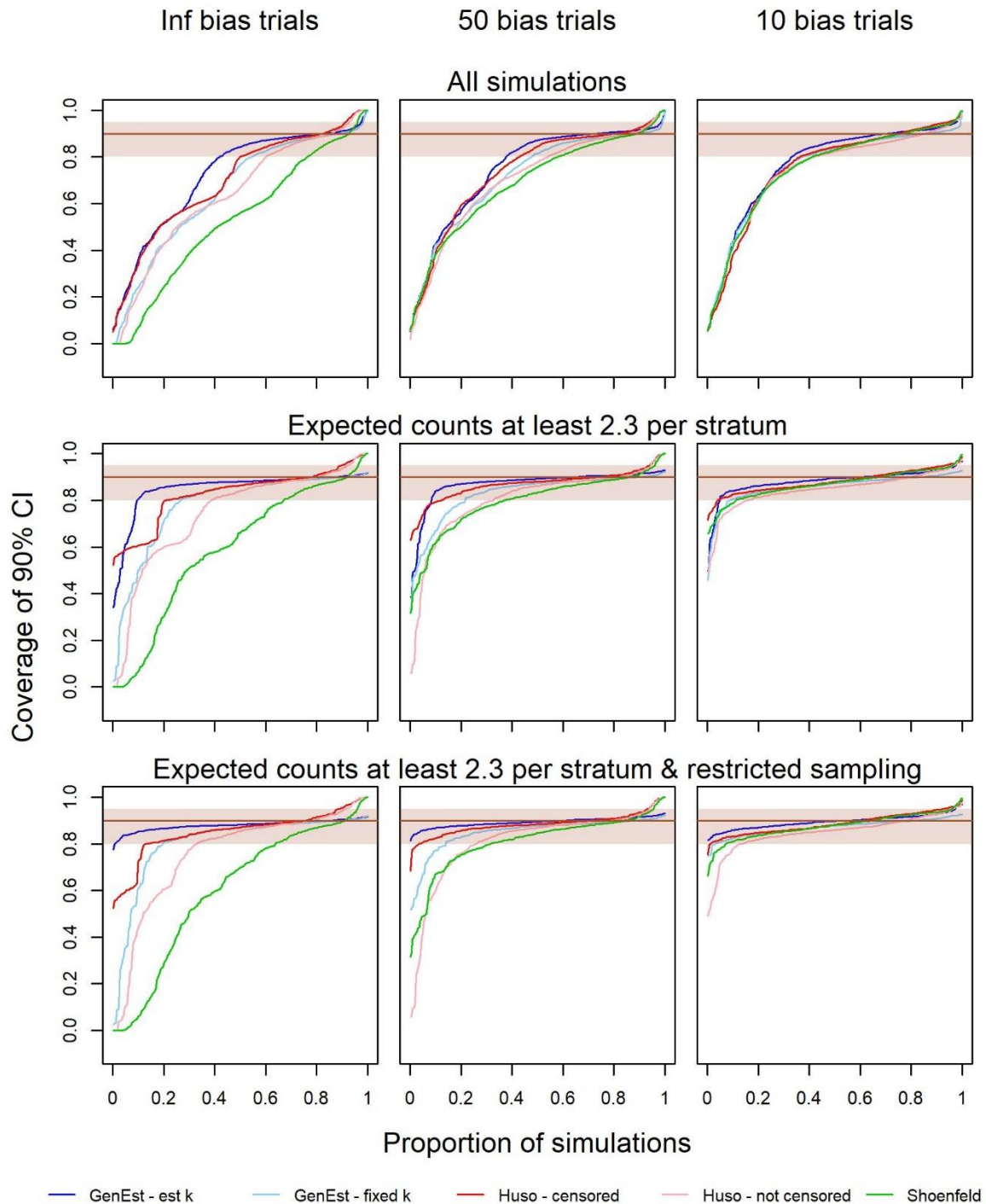


Figure 1. Relative bias of the five estimators under the 36 core scenarios that result in different detection probabilities. Within each panel, the x-axis repeats the  $k$  values twice. The y-axis has been log-transformed so that an underestimate by a factor of 2 is visually similar to an overestimate by a factor of 2. The reference line at 1.0 indicates an unbiased estimator, points above the line suggest estimators that are biased high, and points below the line suggest estimators that are biased low. Dotted reference lines indicate estimates that are 0.8 and 1.2 times the unbiased value.





**Figure 2. Confidence interval (CI) coverage of the five estimators under different bias trial sample sizes (in columns). Within each panel, the realized coverage is plotted from low to high across all simulations we conducted. Nominal coverage is indicated with a brown line at 0.9 and the shaded region includes coverage from 0.8 to 0.95. The top row of panels includes all simulations, the second row excludes simulations for which the expected carcass count was less than 2.3 per stratum (road and pad or cleared plots), and the third row additionally excludes simulations with sampling inadequate to capture the variability in mortality rates across the facility (see text).**

The five estimator variants in Figure 2 are easier to distinguish from one another under the theoretical-ideal case when detection probability is known (i.e. in the left-hand panels), compared to when detection parameters are estimated because there is less “noise.” A second pattern is that as the bias trials use fewer carcasses, the coverages for Shoenfeld, Huso, and GenEst with fixed  $k$  tend to increase because the uncertainties involved in estimating the SE and CP parameters when few trial carcasses are used partially mask the problem of inherent estimator biases.

The top row of Figure 2 includes all simulation conditions and shows that for 30–40% of the simulated conditions, none of the estimators achieved even 80% actual CI coverage with a nominal 90% CI. The *GenEst-est  $k$*  estimator and *Huso-censored* estimators always outperformed the others, followed by the *GenEst-fixed  $k$* , *Huso-not censored*, and *Shoenfeld* estimators. It is important to note that the simulation conditions are not necessarily a representative sample of field conditions, and some were included precisely because they were expected to cause the estimators to fail. The second and third row of panels in Figure 2 sequentially remove some of the most troublesome simulation conditions to illustrate their impact on CI coverage.

All Horvitz-Thompson estimators fail under conditions of very few fatalities or very low detection probability (Korner-Nievergelt et al. 2011) because they all produce estimates of zero mortality with no variance when no carcasses are found. If true mortality is not zero, then these estimates will fail to cover the true mortality, and there is an upper bound on the achievable confidence level. Considering a 90% CI: if there is more than a  $100\% - 90\% = 10\%$  chance that zero carcasses will be detected, it will be impossible to achieve 90% CI coverage with a 90% CI because at least 10% of the time the estimate is zero. It happens that any conditions where the expected average carcass count is less than 2.3<sup>1</sup> are statistically bound to under-cover a nominally 90% CI, and greater confidence levels require greater average carcass counts (a 95% CI requires an expected count of at least 2.99). Further, for data with multiple types of search plots (i.e., groups of plots with different detection probabilities, as occurs in data with some plots searched as road and pads and others with cleared plots), it is necessary that the expected carcass count be at least 2.3 in each type of search plots. Adequate expected carcass counts in all types of search plots are necessary to ensure that the data are balanced in a way that accurately reflects the overall detection probability for the whole study.

The second row of panels in Figure 2 is plotted after excluding all simulation cases for which the expected carcass count is less than 2.3 in any type of search plots. For the ideal case where bias parameters are known (left hand panel), the coverage for *GenEst-est  $k$* , *Huso-censored*, and *GenEst-fixed  $k$*  estimators all improve markedly, *Huso-not censored* improves moderately, and coverage of *Shoenfeld* estimates is nearly unchanged. As bias trial sample size decreases (moving right across the panels), the coverage of the worst-performing estimators increases due to widening CI's and the five estimators behave more similarly to one another, though the rank-order performance (*GenEst-est  $k$*  > *Huso-censored* > *GenEst-fixed  $k$*  > *Huso-not censored* > *Shoenfeld*) is maintained.

---

<sup>1</sup> The probability that a carcass count,  $x$ , is zero, assuming  $x$  is Poisson-distributed with mean 2.3 is 0.10.

Another PCM design condition that can cause problems for estimators is a sampling strategy that is inadequate to capture the variability in mortality from turbine to turbine across the facility. In the simulations presented here, these conditions are present in cases where 1) there were just 10 turbines at the wind facility, 2) a gradient of mortality among the turbines (see Spatial Distribution of Mortality in Table 1), and 3) a sampling fraction of 30% of the turbines (i.e., just 3 turbines). In those cases, the probability of a sample that is not representative of average conditions at the site is high.

The third row of panels in Figure 2 is plotted after excluding cases where the expected carcass count in any stratum was less than 2.3 and excluding cases where there were just 10 turbines at a wind facility with a gradient of mortality among turbines and a 30% sample of searched turbines. In this case, the *GenEst-est k* estimator almost never achieves less than 80% coverage for a nominal 90% CI. To the extent that the *Huso-censored* estimator underperforms *GenEst-est k*, it is due to differences in the way uncertainty in counts is estimated (nonparametric bootstrap versus parametric bootstrap). To the extent that the *GenEst-fixed k* estimator underperforms *GenEst-est k*, it is due to violations of the assumption about the value of *k*. For *Huso-not censored* and *Shoenfeld* estimators, both treatment of uncertainty and violated assumptions contribute to under-coverage.

After eliminating conditions under which no Horvitz-Thompson estimator can achieve good coverage and when only 10 trial carcasses are used to estimate detection parameters, all the estimators achieve coverage close to 90% in > 80% of the remaining cases, but as discussed below, this is at a cost of precision, i.e., wide confidence intervals.

### 3.3 Precision and Confidence Interval Coverage

Precision refers to the dispersion of an estimate around its point value and in this document is assessed as the width of the 90% CI divided by the true mortality—a standardization that facilitates comparisons across scenarios with greatly varying *M*. In general, precision is useless if coverage is poor because an estimate that is tightly constrained around the wrong answer can only mislead. Consequently, precision and coverage are both shown on each figure in this section, and for results with poor coverage, we do not dwell on precision.

Figures 3 through 7 are all formatted similarly. Each figure has five rows of panels with the response of one of the estimators on each row. Each figure has two or three columns of panels that include simulations with one level of a factor, and the x-axis of each panel includes the levels of one or two factors from the simulation. Each panel has two y-axes; the axis on the left indicates relative width of the 90% CI (i.e.,  $\frac{Upper\ bound - Lower\ bound}{M}$ ), and the figures use boxplots to demonstrate the distribution of relative CI widths obtained in the simulations. The right y-axis indicates CI coverage for the simulations with a reference line at the nominal, 90% coverage and asterisks to indicate the coverage obtained in our simulations. The right axis and plotting are in blue to help distinguish them from the relative CI width information.

Precision and coverage were both strongly affected by the level of total mortality at a facility (Figure 3). All five estimators had coverage far below the nominal 90% when total mortality was 10. As discussed in the CI section above, these estimators are not designed to handle rare-event estimation and are known to break down when there are few detections. Consequently,  $M = 10$  cases are not discussed further in this document. Of the five estimators, only the Shoenfeld estimator failed to achieve nominal coverage with  $M = 100$  or 1,000 carcasses, because the simulated carcass removal conditions (Weibull distributed removal times) do not match the assumption inherent in the Shoenfeld estimator (exponentially distributed removal times). For all five estimators, relative precision increased with the total mortality and as the number of bias trial carcasses increased. Higher total mortality reduces the sampling error in the search process, and larger sample sizes for bias trials increases the precision in the bias correction factors, both of which lead to greater precision in the mortality estimates. The increase in precision associated with larger bias trial sample sizes was greater as the effort increased from 10 to 50 carcasses than as the effort increased from 50 carcasses to infinite (which implies bias correction factors are known without error), suggesting diminishing returns as the number of bias trials increases beyond 50.

Among the five estimators, only the Shoenfeld estimates had coverage that was strongly affected by the carcass persistence time distribution (Figure 4). Most Shoenfeld estimates had coverage that was less than nominal when carcass persistence times followed a Weibull distribution because the Weibull-distributed persistence times violate one of the core assumptions for that estimator. Coverage of *Huso-not censored*, *Shoenfeld* and, to a lesser extent, *GenEst-fixed k* estimates was less than nominal when the true value of  $k$  violated the estimators' assumptions (i.e.,  $k = 0$ ,  $k = 1.0$ , or  $k = 0.7$ , respectively). Except for the *Shoenfeld* estimates when carcass persistence time was Weibull distributed, the effect was reduced when  $p = 0.8$  because the influence of  $k$  on detection probability is reduced as  $p$  increases. Coverage of *GenEst-est k* estimates and *Huso-censored* estimates was close to nominal for all combinations of persistence time distribution,  $p$  and  $k$ , because the data that informs those estimates (as gathered for GenEst, or censored for Huso) does not violate any of their core assumptions. All of the estimates summarized in Figure 4 had less precision with lower  $p$  because there is more uncertainty in the final estimate when the detection probability is lower. Most of the estimates summarized in Figure 4 also had less precision with Weibull-distributed carcass persistence time, probably because the particular Weibull distribution we used has more rapid removal of fresh carcasses compared to an exponential distribution with the same mean persistence time, so that the overall detection probability is lower with the Weibull distribution. For estimators with bias that is sensitive to the true value of  $k$ , precision also increased as the true value of  $k$  increased because the precision in an estimate tends to scale with the estimated value of  $M$  rather than the true value of  $M$  (data not shown).

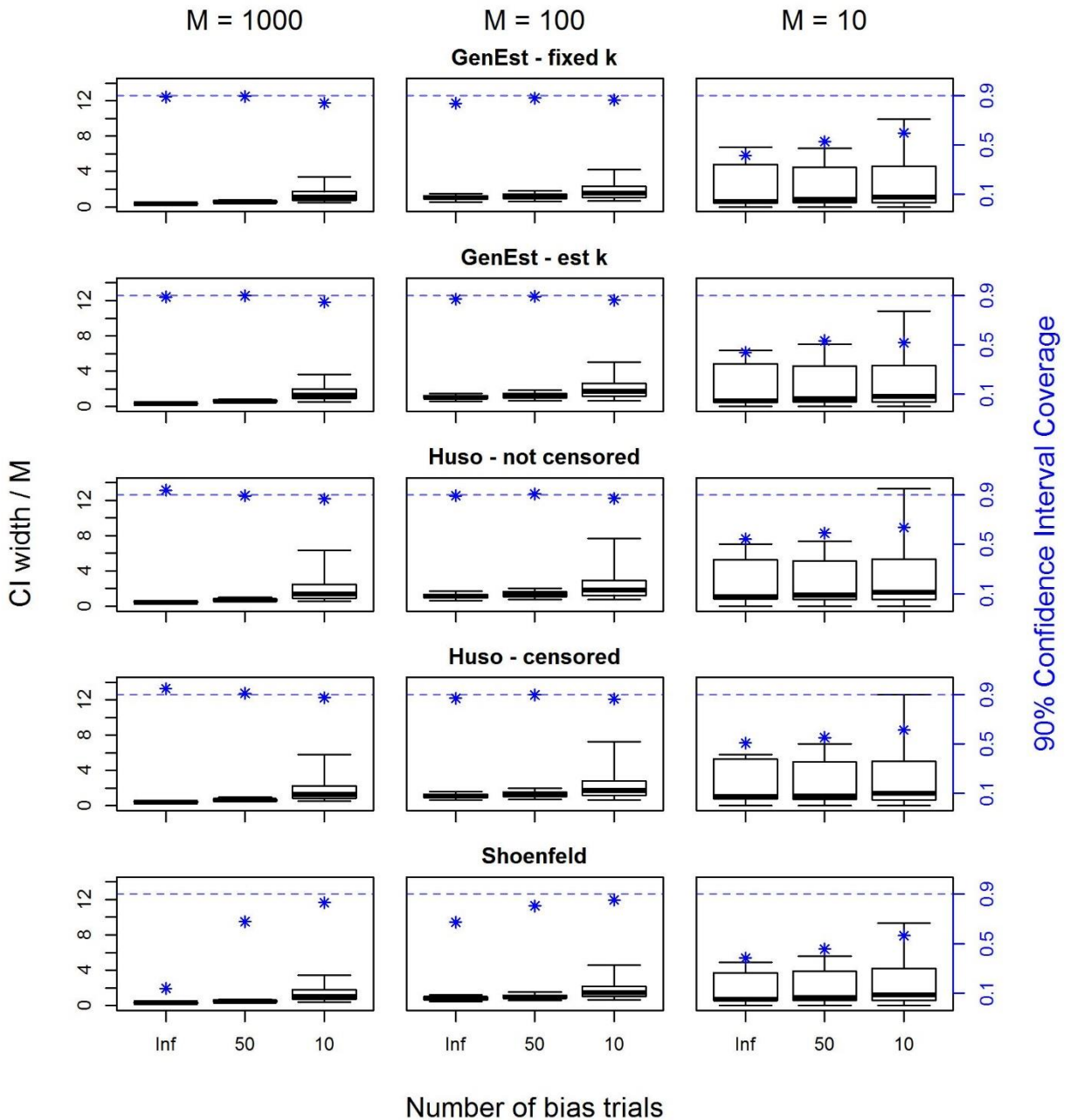


Figure 3. Precision and confidence Interval (CI) coverage of mortality estimates in response to total mortality and sample size for bias trials. Boxplots show the median (horizontal bar), 25<sup>th</sup> and 75<sup>th</sup> quantiles (lower and upper bounds of the boxes) and 5<sup>th</sup> and 95<sup>th</sup> quantiles (whiskers) of the widths of 90% CI for mortality estimates. CI coverage is indicated in blue on the right axis and with asterisks, with a reference line indicating 90% coverage. The figure includes simulations for which there was a gradient of mortality across the 100-turbine wind facility. Sampling fraction was 100% with 30% of turbines searched as cleared plots and 70% as road and pads,  $p = 0.8$ ,  $k = 0.7$ , and carcass persistence was Weibull distributed with mean persistence time equal to the search interval.

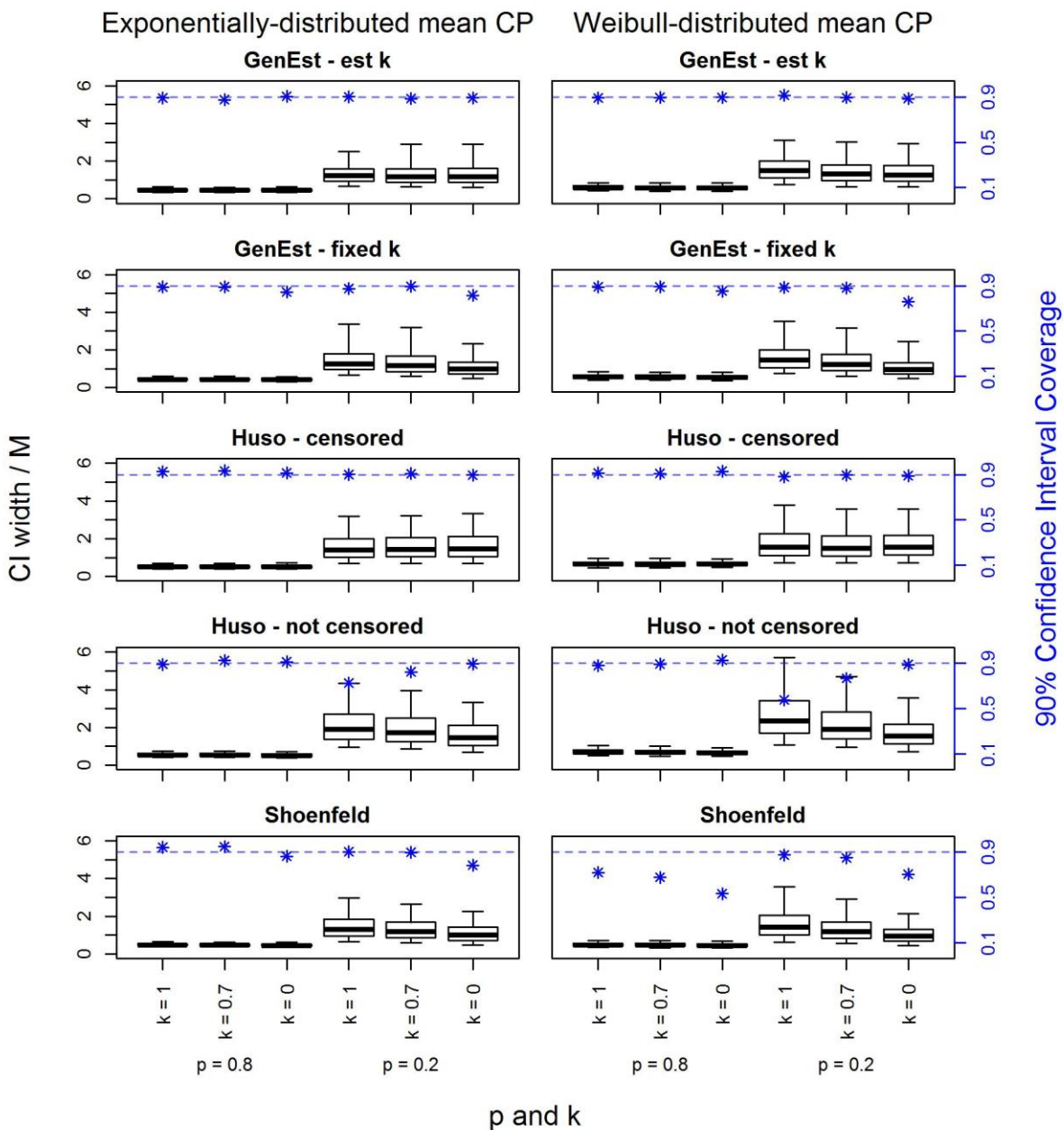


Figure 4. Precision and coverage of mortality estimates due to the carcass persistence time distribution,  $k$  and  $p$ . Boxplot interpretation as in Figure 3. The figure includes simulations for which total fatality was 1,000 individuals with a gradient of mortality across the 100-turbine wind facility. Sampling fraction was 100% with 30% of turbines searched as cleared plots and 70% as road and pads. Mean carcass persistence time was equal to the search interval. There were 50 bias trial carcasses available to estimate model parameters.

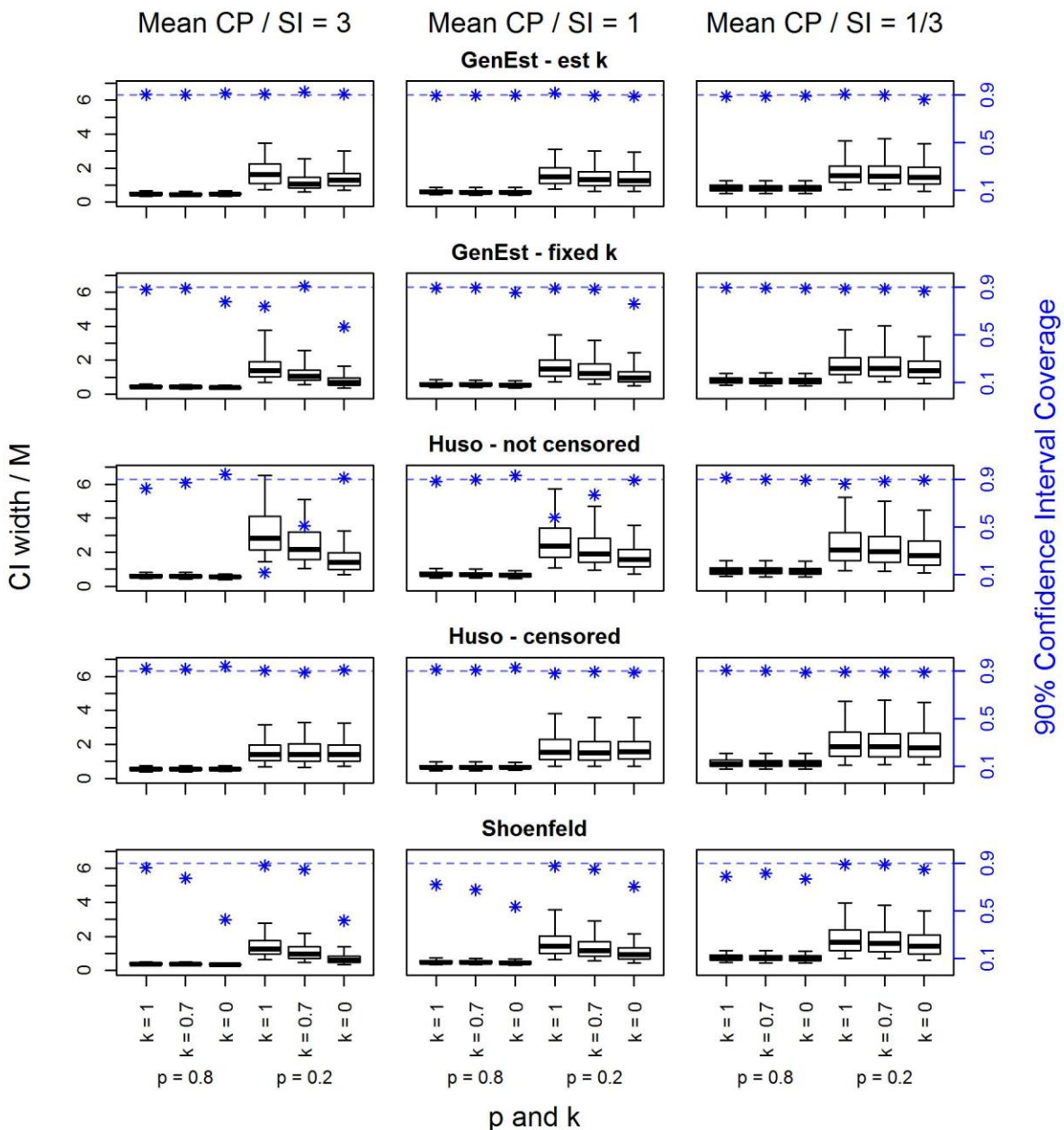


Figure 5. Precision and coverage of mortality estimates due to the length of the mean carcass persistence time relative to the search interval,  $k$  and  $p$ . Boxplot interpretation as in Figure 3. The figure includes simulations for which total fatality was 1,000 individuals with a gradient of mortality across the 100-turbine wind facility. Sampling fraction was 100% with 30% of turbines searched as cleared plots and 70% as road and pads; carcass persistence was Weibull distributed. There were 50 bias trial carcasses available to estimate model parameters.

CI coverage was insensitive to the mean carcass persistence time: search interval ratio for all cases where the value of  $k$  and the removal-time distribution matched the assumptions of the estimator. These cases include *GenEst-est k* (all conditions), *GenEst-fixed k* (when  $k = 0.7$ ), *Huso-not censored* (when  $k = 0$ ), *Huso-censored* (all conditions because censored data match the assumption), but not *Shoenfeld* (due to the mismatch between the Weibull removal time distribution and the *Shoenfeld* assumption of an exponential removal time distribution; Figure 5). Coverage was also relatively insensitive to  $k$  for all estimators when the mean carcass persistence time was short relative to the search interval (i.e., 1/3) because the influence of  $k$  on detection probability is low under conditions when carcasses are likely to be removed before a second search can occur. For the same reason, the influence of  $k$  on coverage for *GenEst-fixed k*, *Huso-not censored*, and *Shoenfeld* was greatest when carcass persistence time was long (i.e., 3) relative to the search interval.

Variable mortality rates between turbines resulted in coverages that deviated from nominal coverage compared to cases where the mortality rate was uniform among turbines (Figure 6). In most cases (*Shoenfeld* excepted; see above), variable mortality rates resulted in modest differences between actual and nominal coverage, except where the monitoring included a 30% sample of 10 turbines (i.e., a sample of just three turbines). In these cases, the coverage was slightly higher for estimators using a non-parametric bootstrap (the two *Huso* estimators and the *Shoenfeld* estimator) compared to the *GenEst* estimators, because the nonparametric bootstrap rolls up some of the turbine-to-turbine count variation in the variability around the  $M$  estimate, whereas the *GenEst* parametric bootstrap does not. Small differences notwithstanding, the coverage with a 3-turbine sample was poor because it is easy with such a small sample to obtain a monitoring data set that is not representative of the overall facility. The risks associated with small sample sizes have long been recognized, which is why the *Comprehensive Guide to Studying Wind Energy/Wildlife Interactions* (Strickland et al. 2011) recommends a sample of at least 10 turbines for PCM studies. The two *Huso* estimators had a slight tendency to over-cover when there was both 100% of turbines surveyed and variation in the mortality rate between turbines, again, because the non-parametric bootstrap tends to include turbine-to-turbine variability in the variation associated with estimated mortality and, so, over-estimates variability when the turbine sample represents a complete census. When all turbines are sampled, including turbine-to-turbine variability in the mortality estimate is inappropriate. Coverage for the *GenEst* and *Huso* estimators was usually close to nominal when mortality rates were uniform among turbines. The *Huso* and *Shoenfeld* estimators had less precision when mortality was not uniform among turbines, and all estimators had less precision with a 30% sample than when 100% of turbines were included in the surveys. Although searching every turbine is a failsafe option, it is not always feasible. When sampling is necessary, these results emphasize the importance of using a sample of turbines that is a good representation of the entire facility.



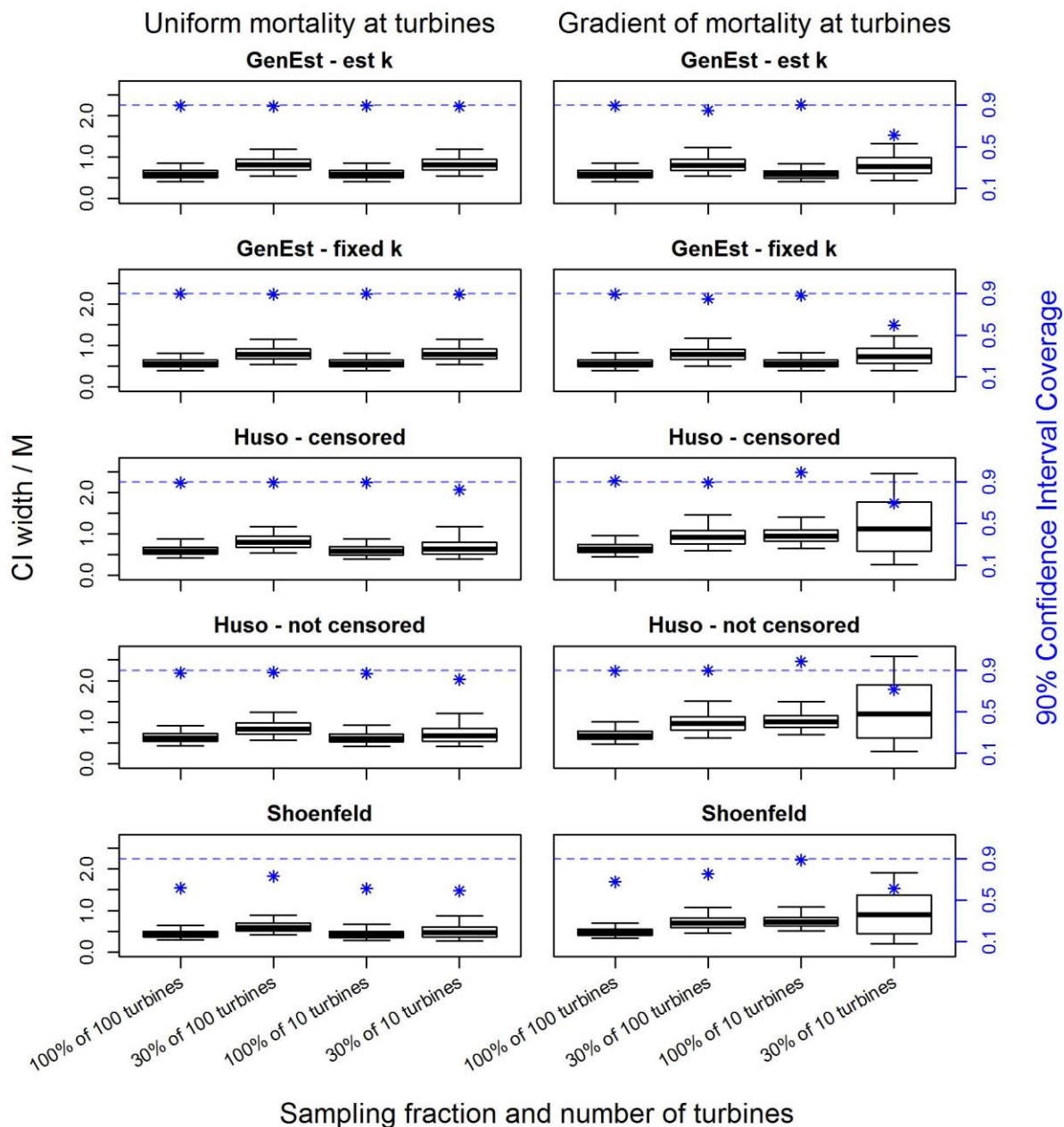


Figure 6. Precision and coverage of mortality estimates due to spatial distribution of fatalities, sampling fraction, and total number of turbines at the facility. Boxplot interpretation as in Figure 3. The figure includes simulations for which total fatality was 1,000 individuals. Thirty percent of searched turbines were searched as cleared plots and 70% as road and pads,  $p = 0.8$ ,  $k = 0.7$ , and carcass persistence was Weibull distributed with mean persistence time equal to the search interval. There were 50 bias trial carcasses available to estimate model parameters.

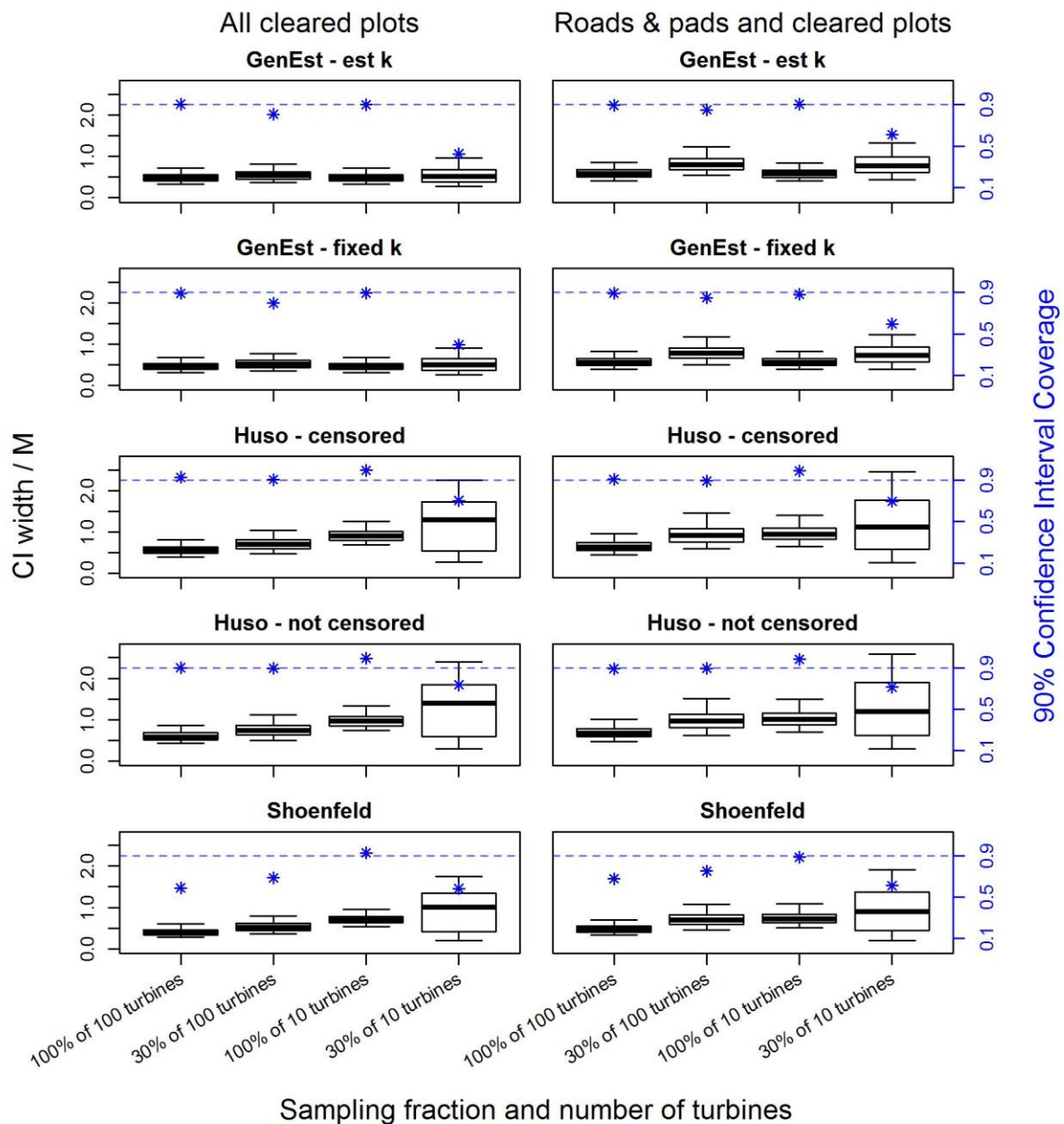


Figure 7. Precision and coverage of mortality estimates due to the plot configuration, sampling fraction, and total number of turbines at the facility. Boxplot interpretation as in Figure 3. The figure includes simulations for which total fatality was 1,000 individuals with a gradient of mortality across the wind facility,  $p = 0.8$ ,  $k = 0.7$ , and carcass persistence was Weibull distributed with mean persistence time equal to the search interval. There were 50 bias trial carcasses available to estimate model parameters.

Plot configurations had little effect on coverage or precision of estimates from any estimator, aside from those already noted to result from lower detection probabilities or low numbers of turbines included in the sample (Figure 7). However, our simulation results should not be taken as an indication that plot configurations are unimportant. We note that in our simulations the area correction associated with road and pads was assumed known without error or uncertainty, but, in practice, area corrections are difficult to estimate and can introduce considerable uncertainty into mortality estimates (though they would do so equally across all of the estimators considered here). The degradation of precision associated with road and pad sampling in Figure 7 is likely understated relative to the results that would be realized if the DWP had to be estimated from data.

## **4 Implications for the Analysis and Design of Post-construction Monitoring Studies**

Key implications for the design and analysis of post-construction monitoring studies

- GenEst is currently the best available statistical mortality estimator
- Study-specific estimates of  $k$  are ideal
- Maintaining high levels of initial searcher efficiency will mitigate cases when  $k$  cannot be estimated, because mortality estimates are less sensitive to  $k$  when initial searcher efficiency is high
- It is essential for study designs to capture a representative sample of the wind facility—no estimator performs well with a poor sample
- Higher sampling fractions may be warranted when the total number of turbines at a facility is low or when there may be a gradient in mortality across the facility
- Mortality estimates and their confidence intervals are unreliable when carcass counts are low (less than three per stratum)
- Low detection probabilities lead to poor precision
- Precision increased notably as bias trial sample size increased from 10 per stratum to 50 per stratum, but there were diminishing benefits beyond 50

*GenEst-est k* and *Huso-censored* are both unbiased estimators across all simulation conditions tested here (Figure 1). *GenEst-est k* outperforms all other estimators in terms of CI coverage across all simulation conditions tested here (Figure 2). Considering just comparisons between estimators that are achieving nominal coverage or close to it, *GenEst-est k* is as precise, or more so, than any of the other estimators (Figures 3–7). By these criteria, *GenEst-est k* should be the clear choice of estimator for the analysis of PCM studies.

By contrast, although the *Shoenfeld* estimator was state-of-the-art when it was first introduced in 2004, it includes strong assumptions and our simulations show that it is biased under a variety of conditions (Figure 1), and does not achieve nominal CI coverage under a variety of conditions (Figure 2). For these reasons, the *Shoenfeld* estimator will not be considered further. Similarly, *Huso-not censored* is sometimes biased (Figure 1) and is much more prone to under-coverage than *Huso-censored* (Figure 2), so it will not be considered further.

Although the purely statistical criteria above point unambiguously to *GenEst-est k*, cost is also a factor in PCM study design, estimating  $k$  can be expensive, and under some conditions (see below) mortality estimates are relatively insensitive to  $k$ . Further, even when PCM data are planned to estimate  $k$ ,  $k$  is a difficult parameter to estimate and the fitting routine sometimes fails. For example, the *GenEst-est k* estimator failed to estimate the  $k$  parameter 39% of the time with 10 bias trials and 11% of the time with 50 bias trail carcasses. In these cases, or when data are not available to estimate the  $k$  parameter, a user has to choose an alternative estimator.

For two reasons, the *GenEst-fixed k* estimator is a better choice than the *Huso-censored* estimator. First, *GenEst-fixed k* can take any value for an assumed  $k$ , and, so, can use the same  $k = 0$  modelling approach as the *Huso-censored* estimator, if desired. Second, our results for the *Huso-censored* estimator are optimistic because we were able to guarantee that the censoring process was perfect. In other words, our virtual searchers were able to discern perfectly whether a carcass was fresh since the prior search or old and had been missed on a prior search. In the field, the potential for systematic errors in the censoring process is much higher. Practitioners should weigh the potential for censoring errors against the impact of mis-specifying an assumed value of  $k$  for *GenEst-fixed k*. The sensitivity of estimates to  $k$  is beyond the scope of these simulations, but interested parties can investigate the effect of the value of  $k$  on mortality estimates at <https://west-inc.shinyapps.io/GenEstSens/>. Under a wide range of conditions, and particularly when  $k$  is difficult to estimate (i.e., fast carcass removal or high initial searcher efficiency), mortality estimates are relatively insensitive to  $k$ .

An important outcome from these simulations is the finding that the *Huso-censored* estimator and *GenEst-est k* are both unbiased (assuming perfect censoring for the former). The practical implication for wind power plant operators is that mortality estimates produced by GenEst should be comparable in magnitude to estimates produced by *Huso-censored*. Practitioners transitioning from Shoenfeld to GenEst (or from Shoenfeld to Huso) should expect to see mortality estimates increase moderately, due to the bias inherent in the Shoenfeld estimator.

In practice, we do not know the true mortality in the field, nor any of the true parameter values for our search process. This simple fact emphasizes the value of an estimator—such as GenEst—that performs well under a wide variety of conditions. In addition, practitioners should be aware of PCM designs that will cause all estimators to fail. Chief among these is the case where carcass detection is a rare event. In our simulations, a threshold of 2.3 expected carcasses per stratum vastly improved the CI coverage of all estimators. A detailed analysis of threshold counts for reliable estimates from GenEst is not yet available, but as an initial heuristic, practitioners should treat estimates based on data with fewer than three carcasses per stratum with caution. Finally, PCM designs need to be adequate to fully represent the variability at the facilities where they are implemented. For facilities with small numbers of turbines, this may mean including a larger fraction of the wind turbines in the sample.

## 5 LITERATURE CITED

- Dalthorp, D., M. M. P. Huso, and D. Dail. 2017. Evidence of Absence (V2.0) Software User Guide. US Geological Survey (USGS) Data Series 1055. USGS, Reston, Virginia. 109 pp. doi: 10.3133/ds1055. Available online: <https://pubs.usgs.gov/ds/1055/ds1055.pdf>
- Dalthorp, D. H., L. Madsen, M. M. Huso, P. Rabie, R. Wolpert, J. Studyvin, J. Simonis, and J. M. Mintz. 2018a. GenEst Statistical Models—a Generalized Estimator of Mortality. US Geological Survey Techniques and Methods, Volume 7, Chapter A2. 13 pp. doi: 10.3133/tm7A2. Available online: <https://pubs.usgs.gov/tm/7a2/tm7a2.pdf>
- Dalthorp, D. H., J. Simonis, L. Madsen, M. M. Huso, P. Rabie, J. M. Mintz, R. Wolpert, J. Studyvin, and F. Korner-Nievergelt. 2018b. Generalized Mortality Estimator (GenEst) - R Code & Gui. US Geological Survey (USGS) Software Release. doi: 10.5066/P9O9BATL. Available online: <https://www.usgs.gov/software/genest-a-generalized-estimator-mortality>
- Dalthorp, D. H., J. Simonis, L. Madsen, M. Huso, P. Rabie, J. M. Mintz, R. Wolpert, J. Studyvin, and F. Korner-Nievergelt. 2018c. GenEst R Package. R Package. Isbn. Accessed May 2020. Information online: <https://cran.r-project.org/web/packages/GenEst/index.html>
- Horvitz, D. G. and D. J. Thompson. 1952. A Generalization of Sampling without Replacement from a Finite Universe. *Journal of the American Statistical Association* 47(260): 663-685. doi: 10.2307/2280784.
- Huso, M. 2011. An Estimator of Wildlife Fatality from Observed Carcasses. *Environmetrics* 22(3): 318-329. doi: 10.1002/env.1052.
- Huso, M., N. Som, and L. Ladd. 2012. Fatality Estimator User's Guide. US Geological Survey (USGS) Data Series 729. Available online: <http://pubs.usgs.gov/ds/729/pdf/ds729.pdf>
- Korner-Nievergelt, F., P. Korner-Nievergelt, O. Behr, I. Niermann, R. Brinkmann, and B. Hellriegel. 2011. A New Method to Determine Bird and Bat Fatality at Wind Energy Turbines from Carcass Searches. *Wildlife Biology* 17: 350-363.
- Madsen, L., D. Dalthorp, M. M. P. Huso, and A. Aderman. 2019. Estimating Population Size with Imperfect Detection Using a Parametric Bootstrap. *Environmetrics* 31(3): doi: 10.1002/env.2603. Available online: <https://onlinelibrary.wiley.com/doi/abs/10.1002/env.2603>
- Shoenfeld, P. 2004. Suggestions Regarding Avian Mortality Extrapolation. Technical memo provided to FPL Energy. West Virginia Highlands Conservancy, HC70, Box 553, Davis, West Virginia, 26260. Available online at: <https://www.nationalwind.org/wp-content/uploads/2013/05/Shoenfeld-2004-Suggestions-Regarding-Avian-Mortality-Extrapolation.pdf>
- Strickland, M. D., E. B. Arnett, W. P. Erickson, D. H. Johnson, G. D. Johnson, M. L. Morrison, J. A. Shaffer, and W. Warren-Hicks. 2011. Comprehensive Guide to Studying Wind Energy/Wildlife Interactions. Prepared for the National Wind Coordinating Collaborative (NWCC), Washington, D.C., USA. June 2011. Available online at: [http://www.batsandwind.org/pdf/Comprehensive\\_Guide\\_to\\_Studying\\_Wind\\_Energy\\_Wildlife\\_Interactions\\_2011.pdf](http://www.batsandwind.org/pdf/Comprehensive_Guide_to_Studying_Wind_Energy_Wildlife_Interactions_2011.pdf)
- US Fish and Wildlife Service (USFWS). 2012. Land-Based Wind Energy Guidelines. March 23, 2012. 82 pp. Available online: [http://www.fws.gov/cno/pdf/Energy/2012\\_Wind\\_Energy\\_Guidelines\\_final.pdf](http://www.fws.gov/cno/pdf/Energy/2012_Wind_Energy_Guidelines_final.pdf)